

# Depth-Resolved Analysis of Biofilms by Photoacoustic Spectroscopy

Thomas Schmid, Larissa Kazarian, Ulrich Panne and Reinhard Niessner †

*Institute of Hydrochemistry, Technical University of Munich, Marchioninistrasse 17, D-81377 Munich, Germany*

A photoacoustic sensor system is presented for depth-resolved analysis of biofilms. The investigation of biofilm growth on the surface of the sensor head showed the potential of Photoacoustic Spectroscopy (PAS) in this area. The increase of biomass was monitored by analysis of the photoacoustic signal amplitudes (wavelength  $\lambda = 550$  nm). The distribution of the organic mass inside the biofilm was derived from absorption profiles, which were calculated from the measured pressure profiles. Wavelength-dependent measurements allowed the determination of absorption spectra. In this way, changes in the composition of the biofilm could be monitored. Measurements with several sensor heads in combination with an optical fiber multiplexer may allow the determination of three-dimensional profiles of biofilms. A new photoacoustic sensor system was set up, which permits the observation of a biofilm at 3 positions in a biofilm reactor.

**(Received June 29, 2000; Accepted October 14, 2000)**

Due to their relevance for the removal of organic water pollutants, biofilms are an important subject for spectroscopic studies. Biofilms can be considered as matrix-enclosed bacterial populations adherent to each other and/or surfaces. The bacterial cells are enclosed in a matrix of extracellular polymer substances (EPS), which mediate the cohesion between the cells and the adhesion to surfaces. Therefore, EPS are of significance for the mechanical stability of the biofilm<sup>1</sup>. The EPS consist mainly of polysaccharides with considerable amounts of other biological macromolecules, like proteins, lipoproteins, and glycoproteins. The biofilm mass is predominantly water (85-95 % wet weight), bacteria ( $10^9$ - $10^{11}$  cells per mL), and EPS (1-2 % wet weight)<sup>2</sup>. Relevant parameters, which have to be monitored in the context of sewage treatment, are the increase (growth), the decrease (sloughing off) and the distribution of the biomass inside the biofilm (thickness between 100 and 300  $\mu\text{m}$ )<sup>3</sup>. The effectiveness of the biofilm, which is determined by the rates of mass transport and chemical reactions, can be estimated by the measurement of depth profiles of water pollutants.

Photoacoustic Spectroscopy (PAS) has been extensively used for nondestructive investigations in chemical, biological and environmental studies<sup>4,5</sup>. PAS is based on the absorption of short laser pulses in the sample. Subsequently, non-radiative relaxation processes convert the absorbed energy into heat. Due to the thermal expansion of the medium, an acoustic wave is generated, which can be detected by a piezoelectric transducer and recorded time-dependent by an oscilloscope. The amplitude  $p$  of the resulting photoacoustic signal  $P(t)$  can be generally described by<sup>5</sup>

$$p \propto \frac{\beta c^2}{C_p} E_0 \mu_a, \quad \text{Eq.(1)}$$

where  $\beta$  is the thermal expansion coefficient,  $c$  is the speed of sound,  $C_p$  is the heat capacity,  $E_0$  is the pulse energy and  $\mu_a$  is the absorption coefficient of the sample.

The time-resolved detection of photoacoustic pulses allows the depth-resolved investigation of the light absorption inside the irradiated sample<sup>6</sup>. The depth  $z$  of an absorbing object in a sample can be calculated as

$$z = c \cdot t, \quad \text{Eq.(2)}$$

where  $t$  is the time delay between the laser pulse and the arrival of the acoustic wave at the sample surface. By Eq.(2), the time-dependent signal  $P(t)$  can be converted into the corresponding depth-dependent signal  $P(z)$ .

## Experimental

### *Experimental Set-up of the Photoacoustic Sensor System*

The experimental set-up is presented in Fig. 1. A dye laser (FL 3002, Lambda Physik, Göttingen, Germany) pumped by a XeCl excimer laser (EMG 201 MSC, Lambda Physik, Göttingen, Germany) is used for excitation. With the laser dye Coumarin 153, the wavelength can be tuned between 520 and 600 nm. The laser pulse energy, which was measured with a pyroelectric detector (Rj-7100, Laser Precision Corp.), varied between 0.3 and 2 mJ depending on the wavelength at a 10 Hz repetition rate.

The laser pulses have an approximate Gaussian temporal light intensity distribution with a full width at half-maximum (FWHM) of  $4.5 \pm 0.1$  ns. The laser light is guided via a quartz-quartz fiber (HCG-MO550T-10, Laser Components) with a diameter of 550  $\mu\text{m}$  to the sensor head, where the sample is irradiated through the base of a transparent prism. The generated pressure pulse (photoacoustic signal) is detected by a piezoelectric poly(vinylidene fluoride) PVDF film, which is coupled to the opposite side of the base in an indirect detection scheme<sup>6</sup>.

The signal from the PVDF film is fed directly into a

† To whom correspondence should be addressed.  
E-mail: R.Niessner@ws.chemie.tu-muenchen.de

preamplifier (Femto Messtechnik, Berlin, Germany) and the amplified output signal is recorded by a digital storage oscilloscope (Tektronix TDS 620) for a period of 1  $\mu$ s. To improve the signal-to-noise-ratio, the signal is averaged over 100 pulses. The averaged PA signal is transferred to a personal computer for further data analysis. The synchronisation of the digital storage oscilloscope with the laser pulse is realized with a signal generator.

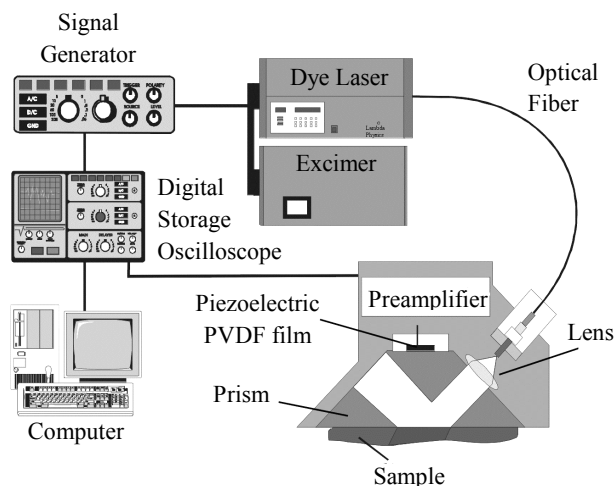


Fig. 1 Experimental set-up of the photoacoustic sensor system.

A more detailed description of the sensor head can be found in <sup>7</sup>. The sensor system allows the depth-resolved analysis of aqueous samples (aqueous solutions, hydrogels and biological tissues) with a depth resolution of about 10  $\mu$ m and a detection limit for the absorption coefficient of 0.02  $\text{cm}^{-1}$  at a laser energy of  $E_0 = 1 \text{ mJ}^8$ .

#### Data Analysis

In aqueous samples, the amplitude of the PA signals depends on the absorption coefficient of the sample, the laser energy, and the temperature. The temperature-dependent parameters in Eq.(1) are  $\beta$ ,  $C_p$  and  $c$ . Under variable conditions (temperature, laser energy), absorption coefficients can be determined, if the PA signals are normalized to well-defined conditions. Different laser energies can be easily corrected due to the linear relationship of the PA signal amplitude and the laser energy. To normalize the PA signal to a certain temperature, literature data for  $\beta$ ,  $C_p$ , and  $c$  was used<sup>8,9</sup>. The "normal" conditions were set arbitrarily to a temperature of 25  $^{\circ}\text{C}$  and a laser energy of 1 mJ for all PA measurements in this study.

The sensor system was calibrated with homogeneous absorbing hydrogel samples. The PA signal amplitudes were plotted as a function of the absorption coefficients, which had been analyzed with an UV/VIS spectrometer (Beckman, Fullerton, CA, USA). Using the following regression function, all measured pressure amplitudes were converted in  $\text{cm}^{-1}$  as the unit of the absorption coefficient<sup>8</sup>:

$$p [\text{kPa}] = 0.144 \text{ kPa cm} \cdot \mu_a [\text{cm}^{-1}] - 0.028 \text{ kPa.} \quad \text{Eq.(3)}$$

The PA signals of homogeneous biofilm samples were plotted as a function of their dry mass. From this followed that a PA amplitude of 1  $\text{cm}^{-1}$  corresponds to approximately 3 % dry mass. Thus, the dry mass of the growing biofilm was estimated.

Depth profiles of the samples could be derived from the photoacoustic signals using an inversion method described in <sup>8</sup>. In that way, the distribution of the absorbed energy inside the sample can be determined.

#### Investigation of a Biofilm Growing on the Sensor Head

The photoacoustic sensor system was used to investigate a biofilm growing on the sensor head. To enhance the adhesion of cells to the prism, the surface of the sensor head was modified with an aminoalkylsilane. *N*-(2-aminoethyl)-3-aminopropylmethylmethoxysilane was dissolved in a mixture of methanol and water (1:1). The surface of the prism was treated with this solution for 12 hours at room temperature.

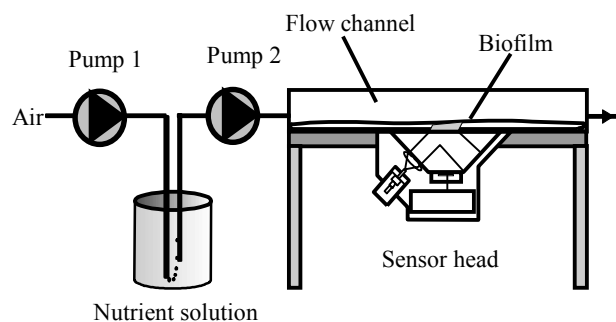


Fig. 2: Experimental set-up for the investigation of a biofilm.

The sensor head was integrated in a flow channel (Fig. 2). A nutrient solution consisting of sodium acetate, yeast extract and inorganic salts (Tab. 1) was pumped through the channel with a volume flow of 35 mL/h (pump 2: MS-Reglo, Ismatec, Wertheim-Mondfeld, Germany). With a volume flow of 500 mL/min, air was pumped into the nutrient solution to obtain aerobic conditions (pump 1: Ecoline VC-280, Ismatec, Wertheim-Mondfeld, Germany). The growth was initialized by addition of a mixture of microorganisms taken from an aerobic sequencing batch biofilm reactor (SBBR).

Tab. 1: Composition of the nutrient solution.

690 mg/L	$\text{NaCH}_3\text{COO}$
60 mg/L	$\text{KH}_2\text{PO}_4$
252 mg/L	$(\text{NH}_4)_2\text{SO}_4$
19 mg/L	KCl
4 mg/L	Yeast extract

## Results and Discussion

#### The Growth of the Biofilm

The biofilm was investigated by photoacoustic measurements twice a day. The absorption of a brown colored biofilm at a wavelength of 550 nm was measured. The increase of the biomass could be monitored by plotting the normalized signal amplitudes as a function of time (Fig. 3). In a first phase, the biomass increased exponentially due to the cleavage of cells. Following, various processes of growth and sloughing occurred, which reached an equilibrium state after 40 days.

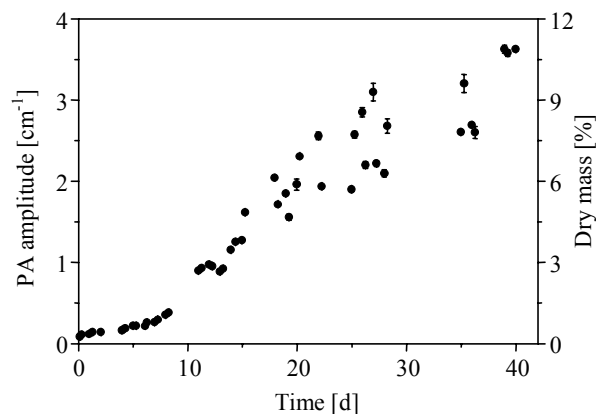


Fig. 3: Growth of a biofilm. Photoacoustic signal amplitudes as a function of time (wavelength  $\lambda = 550$  nm).

#### Distribution of the Biomass Inside the Biofilm

After 8, 27, and 40 days, absorption profiles of the biofilm were derived from measured PA signals. In this way, the distribution of the biomass inside the biofilm could be estimated (Fig. 4). The mass distribution inside the biofilm can be described approximately by an exponential decay starting at the sensor surface. After 40 days, the biofilm reached a dry mass of about 11 % at the sensor surface.

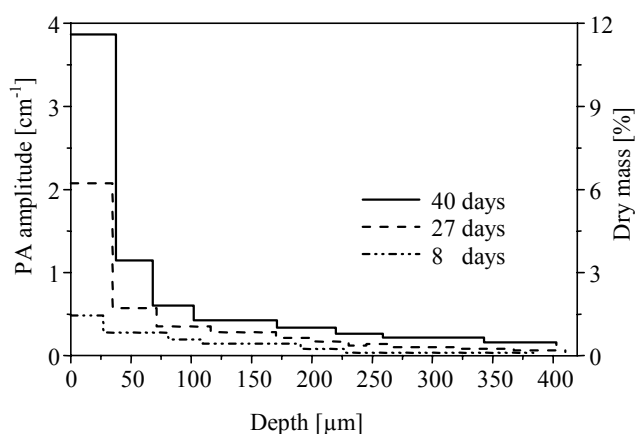


Fig. 4: Absorption profiles of the growing biofilm.

#### Absorption Spectra of the Biofilm

Between day 40 and day 50, the photoacoustic amplitudes were constant. After 50 days, an increase of the measured signal amplitudes could be observed. This was the consequence of a changed composition of the biofilm. Due to the multiplying of a red colored microorganism species, the absorption of the green laser light increased. This could be monitored by the determination of absorption spectra of the biofilm. The wavelength was scanned between 530 and 580 nm in steps of 5 nm and the PA signal amplitudes were plotted as a function of the wavelength. The resulting spectra were compared with the absorption spectrum of the homogeneous biofilm sample, which was used for the initiation of the growth. Thus, the formation of an absorption band at 535 nm could be monitored (Fig. 5).

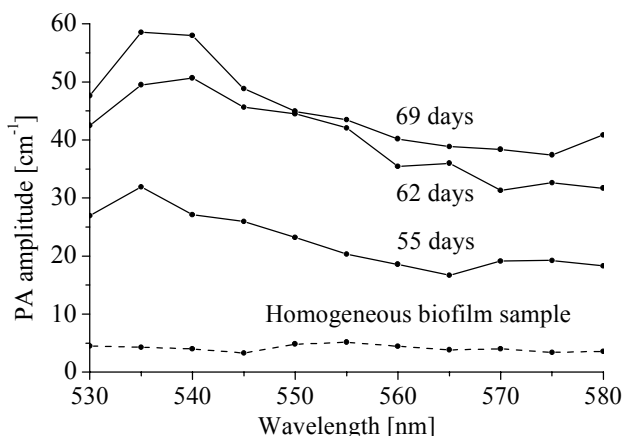


Fig. 5: Absorption spectra of the growing biofilm. For comparison, the spectrum of a homogeneous biofilm sample is shown, which was used for the initiation of the growth.

### Multiplexed Photoacoustic Sensor System

Several photoacoustic sensors are required for an extensive remote sensing of biofilms at different locations in a biofilm reactor. In order to monitor several fiber optically guided sensors with a single laser source and detection unit, an optical switching device – optical fiber multiplexer – is necessary.

#### The Optical Fiber (OF) Multiplexer

In most industrial manufactured OF multiplexers, a switchable fiber is bended<sup>10</sup> or twisted<sup>11</sup> during each switching process either by pivoting or shifting movements. Therewith, the fiber is exposed to bending and torsion moments. A dynamic deformation of a fiber can cause mechanical damage, additional optical performance losses, and change the structure of a transmitted laser pulse. Since the bending radius is continually changing during switching operations, also the corresponding insertion and damping losses change. This reduces the repeatability of the light performance transfer.

A dynamic bending causes massive profile distortion in the fiber due to field distortion. The field offset changes with the alteration of the bending radius with every switching process. This can cause spatial and temporal structural distortions of the laser pulse. However, for time-resolved measurements with photoacoustic sensors an unchanged structure of the transmitted laser pulse with Gaussian distributed energy fluence is required<sup>12</sup>.

The basic principle for the development of the OF multiplexer is the relief of dynamic strain of the optical fiber during the switching processes. The design is based on a transmission fiber connecting the input with the output fiber integrated within a rotary unit. The fiber is completely rotated during the switching processes without dynamic deformation.

The OF multiplexer used in this study had a single optical input port and ten optical output ports. The length of the rotary unit is 55 mm and its diameter 20 mm. The OF multiplexer is driven by a two-phase stepping motor (VEXTA PK245M-01B) with a step resolution of 0.9° and is controlled from a PC by a parallel RS-232 interface. The motor control consists of a parallel interface and a power amplifier. The motor can be set by control to 1/2, 1/4 or 1/8 steps<sup>13,14</sup>.

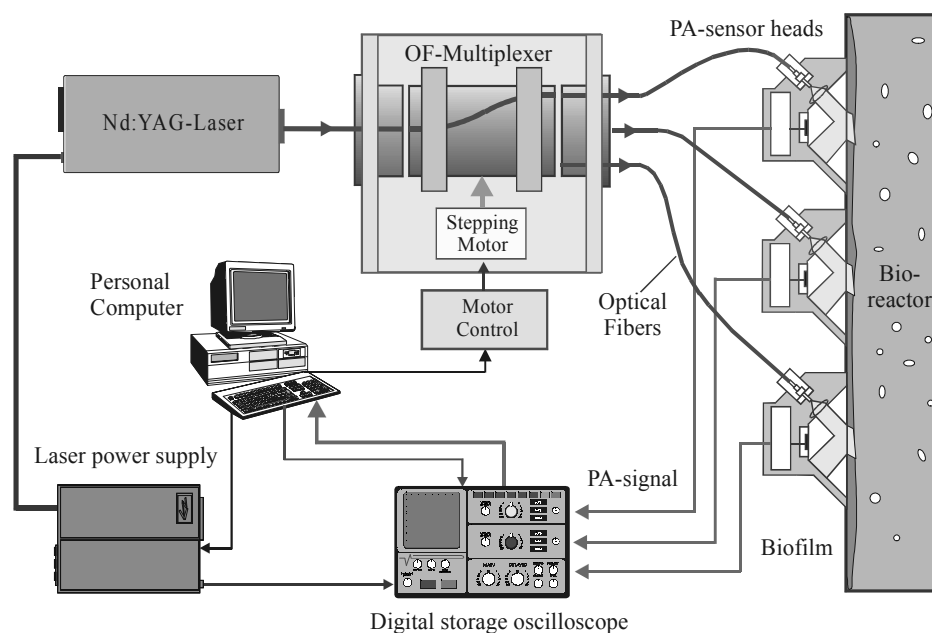


Fig. 6: Multiplexed photoacoustic sensor system.

#### The Multiplexed Sensor System

On the basis of the developed OF multiplexer described above, a sensor system was set up (Fig. 6). In the system as well as in OF multiplexer quartz-quartz fibers (HCG-M0550T-10) with a diameter of 550  $\mu\text{m}$  are used.

For excitation, a Nd:YAG laser (Continuum Surelite I-10,  $\lambda = 532 \text{ nm}$ ) was used. In the OF multiplexer, the light is switched from the optical input port to the selected optical output port. The output ports of the OF multiplexer are connected with the corresponding remote PA sensor heads by optical fibers. The generated PA signals are detected by a piezoelectric film and recorded by a digital storage oscilloscope as described above.

All devices in the measuring system are controlled by one personal computer: the OF multiplexer by a parallel interface, the laser by a serial interface, and the digital storage oscilloscope by an IEEE-488 bus. By the specially developed control program for the software LabView 5.1 (National Instruments Corp.), the number of the chosen output ports (sensor heads), the switching time and in case of repeated measurements also the switching number as well as their sequence are preset. The control program triggers laser power supply and oscilloscope and switches the OF multiplexer (by stepping motor) in such a way that all sensor heads are scanned with preset sequence and frequency.

The indirect detection of the photoacoustic signals allows the integration of sensor heads in the outer wall of biofilm reactors. In that way, the biofilm can be monitored at several positions inside the reactor. The multiplexed photoacoustic sensor system will be used for the investigation of biofilms in a flow channel and a laboratory scale tube reactor with 3 PA sensor heads. On the basis of these model systems, the influence of various process parameters (e.g. pH, temperature, composition of the nutrient solution) on the structure and mechanical stability of the biofilm will be investigated.

#### Acknowledgement

This work was supported by the "Deutsche Forschungsgemeinschaft (DFG)", "SFB 411".

#### References

1. H.-C. Flemming, J. Wingender, R. Moritz, W. Borchard, and C. Mayer, *Spec. Publ. - R. Soc. Chem.*, **1999**, 242, 1-12.
2. J. V. Headley, J. Gandrass, J. Kuballa, K. M. Peru, and G. Yiling, *Environ. Sci. Technol.*, **1998**, 32, 3968-3973.
3. P. A. Wilderer and W. G. Characklis, "*Structure and Function of Biofilms*", **1989**, Wiley and Sons, New York.
4. A. Rosencwaig, "*Photoacoustics and Photoacoustic Spectroscopy*", **1980**, Wiley, New York.
5. A. C. Tam, *Rev. Mod. Phys.*, **1986**, 58, 381-431.
6. A. A. Karabutov, N. B. Podymova, and V. S. Letokhov, *J. Mod. Opt.*, **1995**, 42, 7-11.
7. C. Kopp and R. Niessner, *Appl. Phys. B*, **1999**, 68, 719-725.
8. C. Kopp and R. Niessner, *Anal. Chem.*, **1999**, 71, 4663-4668.
9. R. C. Weast, "*CRC Handbook of Chemistry and Physics*", **1983**, CRC Press, Boca Raton.
10. H. Sakamoto and H. Komazawa, European Patent Application, **1998**, EP 0 846 969 A2.
11. H.-W. Dederichs and T. Ischdonat, German Patent Application, **1996**, DE 195 15 375 A1.
12. C. Kopp and R. Niessner, *Analyst*, **1998**, 123, 547.
13. L. Kasarian and R. Niessner, *Sensors & Actuators A*, **2000**, 84, 250-258.
14. L. Kazarian and R. Niessner, German Patent, **2000**, DE 197 20 619